



RESEARCH ARTICLE

The Protective Effects of Boric Acid against Acrylamide-induced Pulmonary Damage in Rats

Suzan Onur,¹ Mustafa Cengiz^{2*} and Adnan Ayhanci³

¹Faculty of Health Science, Karabuk University, Karabuk, Türkiye; ²Department of Elementary Education, Faculty of Education, Siirt University, Siirt, Türkiye; ³Department of Biology, Faculty of Science, Eskişehir Osmangazi University, Eskişehir, Türkiye

*Corresponding author: m.cengiz@siirt.edu.tr

ARTICLE HISTORY (24-350)

Received: June 23, 2024
Revised: August 2, 2024
Accepted: August 7, 2024
Published online: August 16, 2024

Key words:

Acrylamide
Antioxidant
Biochemical toxicity
Boric acid
Pulmonary damage

ABSTRACT

The purpose of this study was to investigate whether boric acid (BA) can reduce the acute lung injury caused by acrylamide (ACR) in rats. ACR was orally given to produce acute lung damage. Group 1 (saline), Group 2 (ACR, 38.27 mg/kg), Group 3 (20 mg/kg BA), Group 4 (10 mg/kg BA+ACR), and Group 5 (20 mg/kg BA+ACR) were five equal groups of thirty rats. Lungs were taken for histological analysis, immunohistochemical staining and biochemical evaluations after the experimental trial. Malondialdehyde (MDA) levels, a marker of lipid peroxidation and oxidative stress, increased after ACR administration. Nevertheless, it caused the reduction of glutathione (GSH), superoxide dismutase (SOD), glutathione peroxidase (GPx), and catalase (CAT) in lungs. The administration of BA efficiently inhibited the activities of CAT, GSH, SOD, and GPx in lung tissue and protected the lipid peroxidation caused by ACR. Moreover, increased expression of Bax, Caspase-3 and reduced Bcl-2 were found in the lung tissue of rats given ACR, which indicated enhanced congestion, inflammation, alveolar damage, and apoptosis. Interestingly, in rats given ACR injections, BA enhanced the expression of indicators of histological damage and lung injury. These results indicate the efficacy of BA treatment in preventing lipid peroxidation caused by ACR and reducing the negative effects on antioxidant capacity.

To Cite This Article: Onur S, Cengiz M, Ayhanci A, 2024. The protective effects of boric acid against acrylamide-induced pulmonary damage in rats. Pak Vet J, 44(3): 949-953. <http://dx.doi.org/10.29261/pakvetj/2024.229>

INTRODUCTION

Acrylamide (ACR) is a toxic chemical formed by treating high-starch foods (such as French fries, bread and crackers) above 120°C (Exon, 2006; Elsayed *et al.*, 2024). ACR has been recognized and classified as a potential human carcinogen due to its toxic effects including neurotoxic, genotoxic and carcinogenic effects (Becalski *et al.*, 2003; Friedman 2003; Cengiz *et al.*, 2022).

Nature is abundant in boron-containing materials, mostly borate, kernite, colemanite, tourmaline and boric acid (BA) (Cengiz 2018; Cengiz *et al.*, 2019). Because of its water-soluble nature, BA is the most prevalent boron compound in biological systems (Yamada and Eckhart, 2019). Because of its physiological and pharmacological properties, which include antioxidant effects and metabolic modulation, BA has been thoroughly studied for its impact on animal development and reproduction. Research has also demonstrated that BA is protective or therapeutically effective in a variety of pathological conditions including liver damage, cardiac injury, and

testicular damage (Ince *et al.*, 2012; Ayhanci *et al.*, 2020). Nevertheless, little is known about the protective effects of BA on ACR-induced lung injury.

The World Health Organization urges immediate additional study on the health dangers of ACR due to the detrimental impacts of exposure. ACR, an odorless and colorless substance used to synthesize polyacrylamide, is toxic and has wide applications in the textile, paper and cosmetics industries. Tobacco smoke is also one of the main sources of ACR, and is also formed during the high-temperature processing of some foods such as bread, potato chips and crisps (Uthra *et al.*, 2017). In examined animals, ACR can have genotoxic, carcinogenic, developmental, and reproductive effects (ALKarim *et al.*, 2015). According to reports, ACR exposure can lead to significant levels of systemic inflammation and pulmonary impairment in people (Wang *et al.*, 2021). The aim of this study was to find out if BA could safeguard the rat lung tissues against oxidative damage, apoptosis, autophagy, and inflammation caused by ACR.

MATERIALS AND METHODS

Chemicals: ACR (C₃H₅NO, Cas no:79-06-1) was acquired from Sigma-Aldrich Company, while boric acid (H₃BO₃, BA, CAS no: 10043-35-3) was purchased from Chem Pure Private Limited. The remaining substances and reagents utilized in this study were all of analytical or molecular quality.

Animals and study design: This study used male albino rats weighing 250±15 g on an average. All the experimental methods used were approved by the local committee of the Eskişehir Osmangazi University, Türkiye. Stainless steel boxes were used for rearing and the animals were exposed to a 12-hour dark-light cycle, 50±10% relative humidity, and a temperature of 23±10°C. Standard laboratory rodent food was given to the rats, while feed and water were offered ad libitum.

Information on the groups and doses administered to the rat groups (Cengiz *et al.*, 2022) is shown in Table 1. Animals were euthanized under ketamine/xylazine anesthesia and lung tissue was collected. Lung tissue samples were subjected to histologic and immunohistochemical examination.

Lipid peroxidation assay: The assessment of MDA levels was conducted through the thiobarbituric acid-reactive substances assay. Briefly, lung tissue homogenates were subjected to heat treatment with thiobarbituric acid under acidic conditions, resulting in the formation of a pink chromogen, which was then analyzed at a wavelength of 532 nm.

Antioxidant determination: Using SOD (Catalog number: S2515), GPx (Catalog number: D9063), CAT (Catalog number: 219001), and GSH (Catalog number: A5103) assay kits (Randox Lab., Ltd., UK) and the manufacturer's procedure, the activity of these organic compounds in the lung tissue homogenates was ascertained.

Histopathological analysis: Following the dissection of rats, the lungs were carefully removed and cleaned with saline and these tissues were placed into vials containing 10% formalin solution. Following the removal of the tissues, the fixatives were switched, and this procedure was repeated three hours later to improve fixation. Paraffin blocks were made following standard histological tissue examination, and tissue slices measuring 5–6 micrometers thick were stained with hematoxylin-eosin stain and seen under a light microscope. At last, the sections were seen under a light microscope, and an Olympus DP70 camera was used to take pictures. The following scores were applied to H&E-stained slides: (-) no change, (+) modest change, (++) moderate change, and (+++) considerable change for alveolar injury, congestion, inflammation, fibrosis, and necrosis. Rehydrating and deparaffinizing lung tissue slices was a normal procedure. Citric buffer (pH 6.0) was used to accomplish antigen retrieval after sections were cooked in a microwave for ten minutes at 700 W. Primary antibodies against Bax (Abcam, ab53154), Bcl-2 (Abcam, ab196495), and Caspase-3 (Thermo Fischer, CAT: 43-7800) were

incubated on sections after they had been blocked with 3 mL/L H₂O₂ and pig serum, by methodology employed in other investigations. After that, slides were exposed to goat anti-rabbit secondary antibody (EnVision System Horseradish Peroxidase Labeled Polymer; Dako) for 40 minutes at room temperature. This was followed by three further washes with phosphate-buffered saline. After that, slides were counterstained with Mayer's hematoxylin and visualized using a DAB kit (Cengiz *et al.*, 2022).

Statistical analysis: The data was statistically analyzed using SPSS software (Statistics for Windows, IBM Corp, Armonk, NY). One-way ANOVA was used for the analysis of independent measurements and continuous normally distributed data. In addition, the Kruskal–Wallis test was used for the evaluation of the variables with an abnormal distribution. p values less than 0.001 and 0.05 indicated statistical significance in the experimental groups.

RESULTS

Histopathological evaluation: The histological structure of the control group and the BA group were both normal. When comparing the ACR group to the other groups, their histopathology scores were significantly higher (p<0.05). The histopathological scores of the BA+ACR groups were considerably lower (p<0.05) than those of the control, BA, and ACR groups, but there was no difference between them and the BA group (Fig. 1 and Table 2).

Immunohistochemistry: Fig. 2, 3, and 4 show the immunohistochemical evaluation of Bcl-2, Bax, and caspase-3, respectively, in lung sections. In the lung tissues of rats from both the control and BA-only groups, a statistically significant abundance of Bcl-2-positive cells was observed, while the levels of caspase-3- and Bax-positive cells were notably low. Conversely, the lung tissue in the ACR-only group exhibited a substantial increase in the number of Caspase-3- and Bax-positive cells, with a relatively low percentage of Bcl-2-positive cells (p<0.05). A significant decrease in ACR-induced apoptosis was observed in the BA+ACR group, especially in the group given high doses (20 mg/kg) of BA+ACR (p<0.05). In fact, in the BA + ACR combination groups, a decrease in the number of proapoptotic Caspase-3- and Bax-positive cells was observed, while an increase in antiapoptotic Bcl-2-positive cells was detected (p<0.05). In particular, the 20 mg/kg BA+ACR treatment had a more significant antiapoptotic effect (H&E, ×200).

Mean±SD of the five individual observations; + and - indicate the percentage increase and decrease, respectively, compared to the control group. 1: significant difference compared to the normal control group. 2: Significant compared to the ACR-intoxicated group. 3: Significant compared to the ACR+10 mg/kg BA group.

Biochemical parameters: The group that received ACR alone exhibited a significant reduction in GSH levels and CAT, SOD, and GPx activities compared to those in the control group (p<0.001). Additionally, compared with those in the control group, the MDA levels in the ACR group were significantly greater (p<0.001), indicating the occurrence of oxidative stress (Table 3).

Table 1: Lay-out of the experiment.

Number	Group (n=6)	Dose, route, and duration
1.	Control	0.5 mL saline, i.p. once a day for 14 days and sacrificed on the 15 th day
2.	ACR	0.5 mL saline, i.p. once a day for 4 days, 38.27 mg/kg, orally, once a day from day 4 to 14 and sacrificed on the 15 th day
3.	BA	20 mg/kg, i.p. once a day for 14 days and sacrificed on the 15 th day
4.	10 BA+ACR	10 mg/kg, i.p. once on the 14 th day, 38.27 mg/kg, orally, once a day from day 4 to 14 and sacrificed on the 15 th day
5.	20 BA+ACR	20 mg/kg, i.p. once on the 14 th day, 38.27 mg/kg, orally, once a day from day 4 to 14 and sacrificed on the 15 th day

Table 2: The impact of ACR on lung tissue damage and the protective effect of BA were also evaluated across all the experimental groups.

Parameters	Experimental Groups				
	Group 1	Group 2	Group 3	Group 4	Group 5
Congestion	-	-	+++ ¹	++ ^{1,2}	+ ^{1,2}
Inflammation	-	-	+++ ¹	++ ^{1,2}	+ ^{1,2}
Alveolar Damage	-	-	+++ ¹	++ ^{1,2}	+ ^{1,2}
Fibrosis	-	-	++ ¹	- ²	- ²
Necrosis	-	-	++ ¹	+ ^{1,2}	- ²

Note: no change; +, slight change; ++, moderate change; +++, significant change; ¹: significant difference compared to the normal control group. ²: Significant compared to the ACR-intoxicated group.

Table 3: Results of the TBARS (MDA), GSH, SOD, CAT, and GPx activities of the experimental groups.

	MDA (nmol/g tissue)	GSH (nmol/g tissue)	SOD (mU/mg protein)	CAT (U/mg protein)	GPx (mU/mg protein)
1. Control	49,61±3,20	5,06±0,54	11,39±0,60	37,10±1,49	30,51±2,20
2. 20 mg/kg BA	44,52±1,97	5,30±0,25	11,82±0,43	36,96±1,15	30,91±2,26
3. 38.27 mg/kg ACR	105,09±5,24 ¹	2,29±0,25 ¹	5,73±0,45 ¹	21,27±1,18 ¹	15,81±0,79 ¹
4. ACR+10 mg/kg BA	77,72±3,68 ^{1,2}	4,33±0,38 ^{1,2}	7,73±0,65 ^{1,2}	25,09±0,79 ^{1,2}	20,56±1,10 ^{1,2}
5. ACR+20 mg/kg BA	67,09±2,22 ^{1,2,3}	5,23±0,43 ^{2,3}	9,03±0,64 ^{1,2,3}	31,33±2,16 ^{1,2,3}	24,16±1,67 ^{1,2,3}

DISCUSSION

In the present study, biochemical and histopathological analyses were conducted to investigate the influence of BA on ACR-induced lung toxicity in rats. The current study revealed that ACR had the highest MDA levels and the lowest GSH, GPx, CAT, and SOD activity, which depletes cellular antioxidant reserves and causes oxidative stress. Consistent with the literature, a study on ACR-induced liver toxicity found that ACR increased MDA and depleted CAT and SOD (Cengiz *et al.*, 2022). According to findings from another study, ACR inhibits SOD and CAT function and increases oxidative damage by generating oxygen radicals (Jiang *et al.*, 2021). It was used in this study to prove that BA may prevent the decrease in CAT, SOD, GPx, and GSH activities caused by ACR. As compared to the ACR-alone group, the 10 BA+ACR and 20 BA+ACR groups had higher CAT, SOD, GPx, and GSH activities, suggesting that the blood's antioxidant capacity of BA has enhanced. It may be inferred from the literature that BA in this investigation supports antioxidant capability (Ince *et al.*, 2012; Cengiz *et al.*, 2019; Yesildag *et al.*, 2022). Furthermore, the finding of decreased MDA levels in the BA+ACR groups as opposed to the ACR-alone Group in this investigation implies that BA may be able to lessen free oxygen radicals and oxidative stress. Similarly, it has been observed that BA possesses anti-inflammatory and free radical-inhibiting properties (Ayhanci *et al.*, 2020). Other studies in the literature have revealed that BA inhibits the generation of free oxygen radicals in experimental rats with cyclophosphamide-induced kidney damage (Cengiz, 2018) and in rats with ACR-induced liver damage (Cengiz *et al.*, 2022), which is consistent with the results of the current research.

According to Chen *et al.* (2013), ACR increases the activation of caspase and Bax/Bcl-2, which initiates apoptotic pathways. ACR decreased levels of the anti-apoptotic Bcl-2 protein while increasing Bax and caspase-3 (Chen *et al.*, 2013). Conversely, Bax, caspase-3, and anti-

apoptotic Bcl-2 protein expression levels are reversed by BA therapy (Cengiz *et al.*, 2022; Gür *et al.*, 2023; Jabbar *et al.*, 2024). Our results showed that although pro-apoptotic Bax and procaspase-3 expression levels were much greater in ACR compared to other groups, they were still much lower. However, upon administration of ACR/BA combinations, Bax, and caspase-3 levels significantly increased, whereas Bcl-2 levels decreased compared to the ACR-administered group. These findings suggested that ACR could be associated with an increase in apoptotic activity and a decrease in antiapoptotic activity in lung tissue. In the BA+ACR groups, especially in the group in which ACR was administered in combination with a high dose (20 mg/kg) of BA, a significant reduction in ACR-induced apoptosis was observed. Indeed, in the groups where BA+ACR was used together, there was a decrease in the number of proapoptotic caspase-3- and Bax-positive cells and an increase in the number of antiapoptotic Bcl-2-positive cells. The anti-apoptotic impact of BA was more noticeable, particularly when ACR and 20 mg/kg BA were administered together.

It was discovered that ACR caused microscopic degeneration in the lung tissue compared to the other groups. ACR's biochemical and morphological effects on albino rats' lungs were investigated. The study found that inflammation-related symptoms in lung cells, bronchiolar epithelium enlargement, and alveolar epithelium hyperplasia were experienced (Batoryna *et al.*, 2019). Histological degenerations including congestion, inflammation, alveolar damage, fibrosis, and necrosis observed in the ACR group were reduced in the 10 BA+ACR and 20 BA+ACR groups, indicating that BA also improves lung histology.

These findings suggest that using BA may successfully prevent ACR-induced lipid peroxidation and lessen the detrimental effect that it has on the antioxidant system. This study suggested that BA could be a potential new approach for the prevention/treatment of pulmonary toxicity induced by ACR and other lung diseases associated with oxidative stress and inflammation.

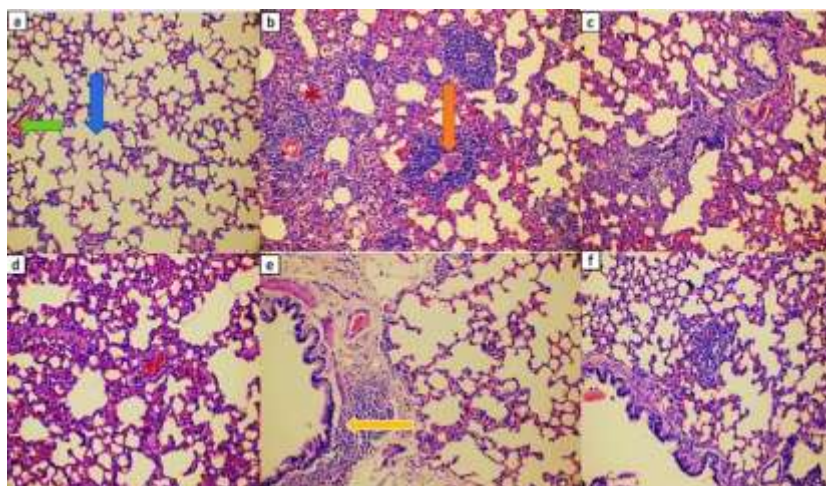


Fig. 1: a: Control group rats' lung parenchyma exhibiting alveoli (blue arrow) and vascular structures (green arrow); b: Rat lung parenchyma following treatment with BA showing degeneration, intense inflammation in the interalveolar area (*), and intense inflammation around vascular structures (orange arrow); c: Rat lung parenchyma following treatment with ACR exhibiting inflammatory cells in the interalveolar area; d: Rat lung parenchyma following treatment with both ACR and BA displaying inflammatory cells in the interalveolar area; e: Rat lung parenchyma following treatment with ACR and BA displaying inflammatory cells in the area around bronchioles (yellow arrow); f: Inflammatory cells in the area around bronchioles in the rat lung parenchyma (H&E, X200).

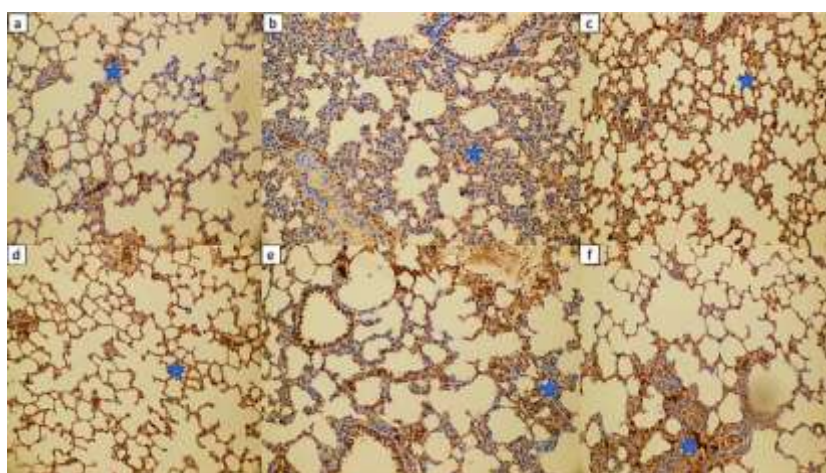


Fig. 2: a: Control group lung parenchyma of rats showing mild gray-brown staining (blue star); b: Rat lung parenchyma following treatment with BA displaying extensive areas of mild yellow-brown staining (blue star); c: Rat lung parenchyma following treatment with ACR showing moderate-intensity yellow-brown staining (blue star); d: Rat lung parenchyma following treatment with both ACR and BA demonstrating moderate-intensity yellow-brown staining (blue star); e: Rat lung parenchyma following treatment with both ACR and BA displaying focal areas of moderate-intensity yellow-brown staining (blue star); f: Lung parenchyma of rats showing mild-to-moderate-intensity yellow-brown staining (blue star) (Bax; X200).

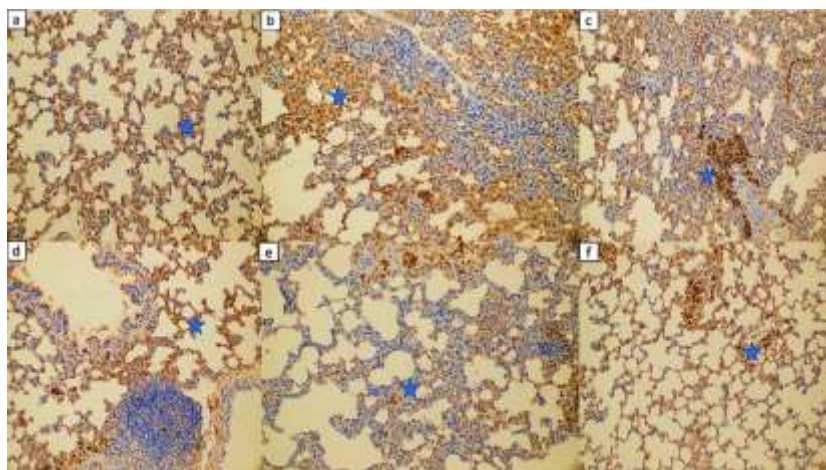


Fig. 3: a: Control group rats' lung parenchyma showing mild gray-brown staining (blue star); b: Rat lung parenchyma following treatment with BA displaying moderate-intensity yellow-brown staining in extensive areas (blue star); c: Rat lung parenchyma following treatment with ACR showing strong intense staining in focal areas and mild-intensity staining in broad areas of yellow-brown color (blue star); d: Rat lung parenchyma following treatment with both ACR and BA exhibiting moderate-intensity yellow-brown staining (blue star); e: Rat lung parenchyma following treatment with both acrylamide and boron displaying mild-intensity yellow-brown staining (blue star); f: Lung parenchyma of rats showing mild-to-moderate-intensity yellow-brown staining (blue star) (Bcl-2; X200).

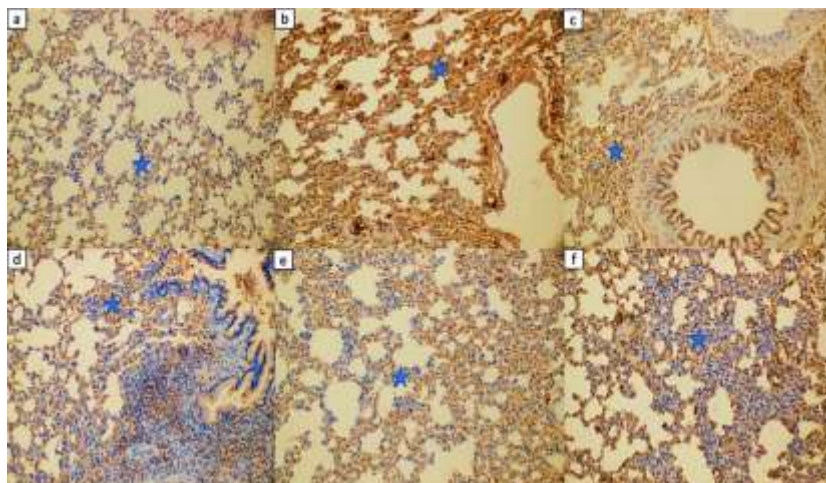


Fig. 4: a: Control group rats' lung parenchyma exhibiting mild gray-brown staining (blue star); b: Rat lung parenchyma following treatment with BA displaying strong yellow-brown staining in extensive areas (blue star); c: Rat lung parenchyma following treatment with ACR exhibiting strong staining in focal areas and moderate staining in broad areas of yellow-brown color (blue star); d: Rat lung parenchyma following treatment with both ACR and BA displaying mild staining of yellow-brown color (blue star); e: Rat lung parenchyma following treatment with both ACR and BA exhibiting mild to moderate staining of yellow-brown color (blue star); f: Lung parenchyma of rats exhibiting mild to moderate staining of yellow-brown color (blue star) (Caspase 3; X200).

Conclusions: The protective effects of BA against the adverse effects induced by ACR, especially those related to lung damage, have not been sufficiently documented in animal experiments. According to our experimental findings, the protective effects of BA may be attributed to its ability to scavenge free radicals, act as a chelating agent, and/or stimulate detoxification enzymes. When the bioavailability of BA, or similar chelating agents, is enhanced through new strategies or technologies, it may provide better protection against ACR-induced lung damage. Despite the potential of chelating agents such as BA to mitigate multiorgan toxicity, current research on this topic is relatively limited.

Authors contributions: Suzan Onur (methodology), Mustafa Cengiz, and Adnan Ayhanci, designed the experimental protocol and original draft preparation, review, and editing. All authors read, revised, and approved the final manuscript.

Ethics approval: An experimental study was conducted with the approval of the Animal Experiments Local Ethics Committee of Eskişehir Osmangazi University (No: 806-2/2023).

REFERENCES

- ALKarim S, ElAssouli S, Ali S, *et al.*, 2015. Effects of low dose acrylamide on the rat reproductive organs structure, fertility, and gene integrity. *Asian Pac J Reprod* 4: 179-187.
- Ayhanci A, Tanriverdi DT, Sahinturk V, *et al.*, 2020. Protective effects of boron on cyclophosphamide-induced bladder damage and oxidative stress in rats. *Biol Trace Elem Res* 197: 184-191.
- Batoryna M, Semla-Kurzawa M, Zyśk B, *et al.*, 2019. Acrylamide-induced alterations in lungs of mice in relation to oxidative stress indicators. *J Environ Sci Heal B* 54: 745-751.
- Becalski A, Lau BPY, Lewis D, Seaman SW, 2003. Acrylamide in Foods: Occurrence, Sources, and Modeling. *J Agric Food Chem* 51: 802-808.
- Cengiz M, 2018. Boric acid protects against cyclophosphamide-induced oxidative stress and renal damage in rats. *Cell Mol Biol* 64: 11-14.
- Cengiz M, Ayhanci A, Akkemik E, *et al.*, 2022. The role of Bax/Bcl-2 and Nrf2-Keap-1 signaling pathways in mediating the protective effect of boric acid on acrylamide-induced acute liver injury in rats. *Life Sci* 307: 120864.
- Cengiz M, Cetik Yildiz S, Demir C, *et al.*, 2019. Hepato-preventive and anti-apoptotic role of boric acid against liver injury induced by cyclophosphamide. *J Trace Elem Med Biol* 53: 1-7.
- Chen JH, Yang CH, Wang YS, *et al.*, 2013. Acrylamide-induced mitochondria collapse and apoptosis in human astrocytoma cells. *Food Chem Toxicol* 51: 446-452.
- Elsayed A, Aboubakr M, Hassan FVV, *et al.*, 2024. Testicular injury of acrylamide in rats and potential protection of coenzyme Q10 and rosuvastatin. *Pak Vet J* [http://dx doi org/1029261/pakvetj](http://dx.doi.org/1029261/pakvetj).
- Exon J, 2006. A review of the toxicology of acrylamide. *J Toxicol Environ Heal B* 9: 397-412.
- Friedman M, 2003. Chemistry, Biochemistry, and Safety of Acrylamide. A Review. *J Agric Food Chem* 51: 4504-4526.
- Gür F, Cengiz M, Gür B, Cengiz O, *et al.*, 2023. Therapeutic role of boron on acrylamide-induced nephrotoxicity, cardiotoxicity, neurotoxicity, and testicular toxicity in rats: Effects on Nrf2/Keap-1 signaling pathway and oxidative stress. *J Trace Elem Med Biol* 80: 127274.
- Ince S, Keles H, Erdogan M, *et al.*, 2012. Protective effect of boric acid against carbon tetrachloride-induced hepatotoxicity in mice. *Drug Chem Toxicol* 35: 285-292.
- Jabbar AA, Alamri ZZ, Abdulla MA, *et al.*, 2024. Boric acid (Boron) attenuates AOM-induced colorectal cancer in rats by augmentation of apoptotic and antioxidant mechanisms. *Biol Trace Elem Res* 202: 2702-2719.
- Jiang G, Lei A, Chen Y, *et al.*, 2021. The protective effects of the Ganoderma atrum polysaccharide against acrylamide-induced inflammation and oxidative damage in rats. *Food Funct* 12:397-407.
- Uthra C, Shrivastava S, Jaswal A, *et al.*, 2017. Therapeutic potential of quercetin against acrylamide induced toxicity in rats. *Biomed Pharmacother* 86: 705-714.
- Wang B, Wang X, Yang S, *et al.*, 2021. Acrylamide exposure and pulmonary function reduction in general population: The mediating effect of systemic inflammation. *Sci Total Environ* 778: 146304.
- Yamada KE and Eckhert CD, 2019. Boric Acid Activation of eIF2 α and Nrf2 Is PERK Dependent: a Mechanism that Explains How Boron Prevents DNA Damage and Enhances Antioxidant Status. *Biol Trace Elem Res* 188: 2-10.
- Yesildag K, Erozu R, Genc A, *et al.*, 2022. Evaluation of the protective effects of morin against acrylamide-induced lung toxicity by biomarkers of oxidative stress, inflammation, apoptosis, and autophagy. *J Food Biochem* 46: e14111.